Sensors and Actuators B xxx (2011) xxx–xxx

Contents lists available at ScienceDirect

Sensors and Actuators B: Chemical

journal homepage: www.elsevier.com/locate/snb

A hybrid chemiresistive sensor system for the detection of organic vapors

Jisun Im[a], Sandip K. Sengupta[a], Maor F. Baruch[a], Christopher D. Granz[b], Srikanth Ammu[c], Sanjeev K. Manohar[c], James E. Whitten[a,*]

[a] Department of Chemistry and Center for High-Rate Nanomanufacturing, The University of Massachusetts Lowell, Lowell, MA 01854, USA
[b] Department of Electrical and Computer Engineering, The University of Massachusetts Lowell, Lowell, MA 01854, USA
[c] Department of Chemical Engineering, The University of Massachusetts Lowell, Lowell, MA 01854, USA

ARTICLE INFO

Article history:
Received 30 November 2010
Received in revised form 2 February 2011
Accepted 14 February 2011
Available online xxx

Keywords:
Chemiresistor
Electronic nose
Gas sensing
Gold nanoparticle
Poly(3-hexylthiophene)
Polypyrrole

ABSTRACT

A five node sensor array, consisting of three films of gold nanoparticles functionalized with *p*-terphenylthiol, dodecanethiol and mercapto-(triethylene glycol) methyl ether, and films of poly(3-hexylthiophene) and polypyrrole, was integrated into a portable, microprocessor-based system. The system was evaluated for the detection of chloroform, diisopropyl methylphosphonate (DIMP), ethanol, hexane, methanol, and toluene vapors. Direct comparison of the five sensor films with respect to sensitivity, response time and recovery time was made by measurement of the resistance changes upon simultaneous exposure to each analyte. In general, the sensor films responded, with greatest sensitivity, to organic analyte molecules with similar chemical functionality (e.g., polarity). For example, the dodecanethiol-functionalized gold nanoparticle film sensor excelled at detecting hexane, while the mercapto-(triethylene glycol) methyl ether-functionalized nanoparticle film exhibited superb detection of ethanol and chloroform. Although the poly(3-hexylthiophene) film was very sensitive to polar analytes, including DIMP, in many cases it suffered from relatively long recovery times. Following training of the sensor system, successful differentiation and detection of the analytes were realized using a relatively simple algorithm based on "minimization of the squares of differences" method. The ability of the system to optimally differentiate these analytes is considered within the context of principal component analysis, and the effects of long-term sensor drift are discussed.

© 2011 Published by Elsevier B.V.

1. Introduction

Electronic noses ("enoses") utilize a quasibiomimetic approach of combining the output signals of arrays of moderately selective, and hence cross-reactive, chemical sensors with data analysis software to improve the selectivity of sensor systems; they can be utilized to identify and possibly quantify different chemical substances in the vapor phase [1]. Chemiresistive materials have been employed to detect toxic chemicals and explosives and have been shown to be suitable for electronic nose applications. While an extensive review is beyond the scope of this discussion, examples of sensing materials include metal oxides [2,3], phthalocyanines [4], conjugated polymers [5–8], conducting element/polymer composites [9–13], silicon nanoribbons [14,15], and thiol-monolayer protected gold nanoparticles [16–25]. Sensor systems based on metal oxides and/or conducting polymers have been commercialized [26], and a hand-held prototype based on thiol-monolayer protected gold nanoparticle films was developed by Wohltjen and Snow in 1999 [27]. A more recent review [28] shows a fair number of commercial enose devices, some produced in volume, being utilized for a variety of applications. Despite the efforts of many research groups, challenges still remain related to selectivity, sensitivity, and stability.

Functionalized gold nanoparticle films generally exhibit fast and reversible responses to volatile organic compounds (VOCs). The response depends, in part, on the partition coefficient [29] between the solid and vapor, and this is determined by the nature of the ligand. In principle, films made from gold nanoparticles functionalized with different ligands could be used to fabricate cross-reactive arrays for enose applications. This solves the problem that a particular gold nanoparticle film responds to multiple VOCs, with one sensor film not being sufficient to identify and quantify an unknown analyte. Adding a variety of distinctly different types of sensors to such an array, forming a so-called hybrid sensor system [30], should, in principle, lead to increased selectivity and better overall sensitivity.

In this study, we have developed a hybrid sensor array consisting of three different thiol-protected gold nanoparticles and two conjugated polymers in order to enhance the system's ability to differentiate various analytes. In the case of gold nanoparticle films, selectivity can be tailored by varying the thiol ligands; for conjugated polymers, the choice of conjugated polymer affects

* Corresponding author. Tel.: +1 978 934 3666; fax: +1 978 934 3013.
E-mail address: James_Whitten@uml.edu (J.E. Whitten).

0925-4005/$ – see front matter © 2011 Published by Elsevier B.V.
doi:10.1016/j.snb.2011.02.025

Table 1
Properties of the five sensor films.

Channel	Sensor	Core size[a] (nm)	Interparticle[a] distance (nm)	Film thickness[b] (nm)	Conductivity (S/cm)
1	3EG-AuNPs	4.9 (±1.3)	1.5 (±0.3)	58.1	2.97×10^{-5}
2	DDT-AuNPs	4.3 (±0.6)	1.3 (±0.3)	26.2	1.09×10^{-7}
3	TPT-AuNPs	3.3 (±0.7)	1.3 (±0.3)	337	5.75×10^{-4}
4	PPy	–	–	17.4	4.21×10^{-3}
5	P3HT	–	–	56.0	3.02×10^{-5}

[a] Core sizes and interparticle distances were measured using TEM, and the value in parenthesis is one standard deviation. The average values were obtained from 45 nanoparticles, in all cases.
[b] The film thickness was measured using AFM.

response to a particular analyte. Unlike metal oxide chemiresistors, all of the sensors in our array operate at ambient temperature, and hence power consumption is very low. In order to evaluate the sensor array containing five chemiresistive materials, a portable, battery-operated, microprocessor-based prototype sensor system, nicknamed "the Mini-Mutt" has been constructed. While the hardware and software used are not at the stage of commercialization, the prototype permits qualitative and quantitative identification of an unknown chemical vapor based on a library of responses and demonstrates the potential of such an instrument. In this paper, we describe the fabrication, calibration, and testing of the hybrid sensor array with respect to sensitivity, selectivity, response time, recovery time, long-term stability, and potential portability. These studies provide direct comparison, by simultaneous measurements, of the performance of three differently functionalized gold nanoparticle and two conjugated polymer films.

2. Experimental

2.1. Materials

p-Terphenylthiol (TPT) was purchased from Frinton Laboratories (Vineland, NJ). 1-Mercapto-(triethylene glycol) methyl ether functionalized gold nanoparticles (3EG-AuNPs), dodecanethiol functionalized gold nanoparticles (DDT-AuNPs), regioregular poly(3-hexylthiophene) (P3HT, greater than 90% head-to-tail fraction), hydrogen tetrachloroaurate (III), tetraoctylammonium bromide, and sodium borohydride were purchased from Sigma–Aldrich. Chloroform, ethanol, hexane, methanol, and toluene, which were used as analytes for sensor measurements, were also obtained from Sigma–Aldrich. Diisopropyl methylphosphonate (DIMP) was purchased from Alfa Aesar. All reagents were of analytical grade and used as received.

2.2. Synthesis and characterization of sensing materials

The synthesis of TPT-protected gold nanoparticles was carried out using the Brust method [31]. Briefly, hydrogen tetrachloroaurate (III) ($HAuCl_4$) was used as a precursor. A phase transfer agent, tetraoctylammonium bromide ($(C_8H_{17})_4NBr$, 1.093 g, 2 mmol), was transferred to an aqueous solution of $HAuCl_4$ (0.3 g, 0.9 mmol), and the mixture was stirred for 20 min. A solution of TPT (78.71 mg, 0.3 mmol) in toluene was added as the stabilizing ligand, and an aqueous solution of sodium borohydride ($NaBH_4$, 0.374 g, 9.88 mmol) was then added drop-wise. The mixture was stirred vigorously for 12 h, and the functionalized nanoparticles were recovered from the organic phase. The gold–sulfur thiolate bond of the TPT-protected gold nanoparticles was confirmed using X-ray photoelectron spectroscopy (XPS) from a drop-cast film. The size distribution of gold nanoparticles was measured using transmission electron microscopy (TEM). Polypyrrole (PPy) nanofibers were synthesized following the procedure described previously [32], and aqueous 1 M HCl was used as a dopant; P3HT was used as-received, without doping.

2.3. Preparation of sensor films and conductivity measurement

All sensor films were prepared by depositing them onto cleaned interdigitated array (IDA) microelectrodes (M1450110, Microsensor Systems, Inc.). These consisted of 50 pairs of gold electrodes with the following dimensions: 15 μm electrode width, 15 μm spacing, 4800 μm overlap length, and 150 nm electrode thickness. Gold nanoparticle films were prepared by drop-casting 2 mg/ml solutions onto the IDA microelectrodes. The PPy and P3HT films were spin-coated onto the microelectrodes using acetone and chloroform solvents, respectively. The five sensor films, consisting of 3EG-AuNP, DDT-AuNP, TPT-AuNP, PPy, and P3HT films, were then installed into a custom-built chamber ($W \times L \times H = 5.5\,cm \times 9.0\,cm \times 2.3\,cm$, $V = 114\,cm^3$) fitted with hermetically sealed electrical feedthroughs, for making connections to the IDAs, and inlet and outlet gas Swagelok fittings.

Conductivity (σ) was calculated using the following equation:

$$\sigma = \frac{d}{(2n-1)LhR} \quad (1)$$

where d is the electrode spacing, n is the number of electrodes, L is their overlap length, h is the film thickness, and R is the film resistance. The resistance values of the films were measured using the two-probe method at room temperature. Properties of the sensor films are shown in Table 1. Resistance values of the 3EG-AuNP, DDT-AuNP, TPT-AuNP, PPy, and P3HT films were 183 kΩ, 111 MΩ, 3.66 kΩ, 4.30 kΩ, and 187 kΩ, respectively. Eq. (1) is valid when the thickness of the film does not exceed that of the gold electrodes. This is not the case for the TPT-AuNP film, and the electrode thickness (150 nm) was used to calculate the conductivity under the assumption that the portion of the film on top of the electrodes contributes negligibly.

2.4. Sensor response measurements and portable prototype sensor system

The electrical resistance changes of the sensor array were measured by exposing it to different concentrations of methanol, ethanol, chloroform, toluene, hexane, and a nerve agent simulant, diisopropyl methylphosphonate (DIMP). Fig. 1 shows a schematic of the vapor delivery and sensor array systems. Vapor streams of varying concentration were generated by bubbling dry nitrogen gas through the analyte of interest and mixing the saturated vapor with pure dry nitrogen gas. These were admitted to the chamber via stainless steel tubing, with the flow rates of the saturated and pure gases controlled and monitored by mass flow controllers (PNeucleus Technologies, Microflo) and mass flow meters(PNeucleus Technologies, MicroMeter). The total flow rate of the vapor stream was kept at 400 sccm. Concentrations were calculated from the partial pressures of the saturated vapors at 25 °C. For these measurements, a DC bias of 200 mV was applied. A low bias voltage was used because of sensor stability [33] and noise [29] considerations.

The prototype of the sensor system consisted of three main parts: a microprocessor board, current-to-voltage circuits inter-

Please cite this article in press as: J. Im, et al., A hybrid chemiresistive sensor system for the detection of organic vapors, Sens. Actuators B: Chem. (2011), doi:10.1016/j.snb.2011.02.025

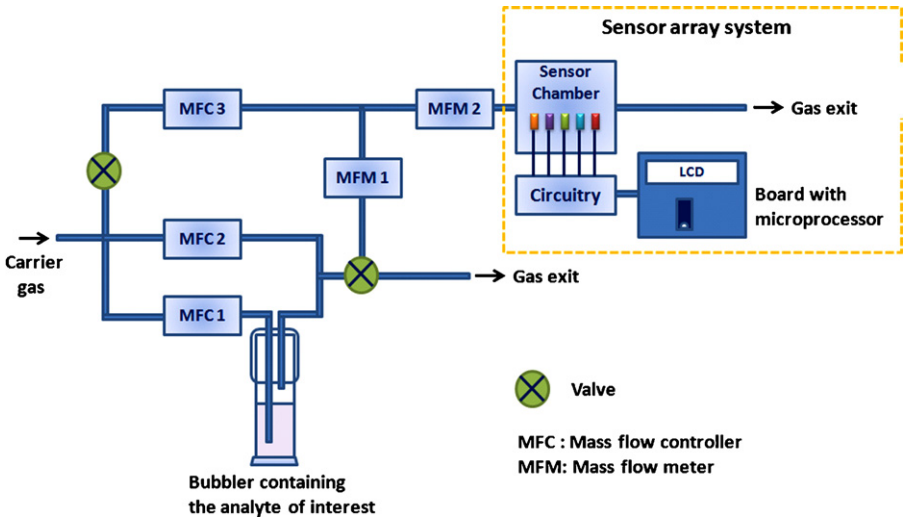

Fig. 1. Schematic illustration of the prototype sensor array system and vapor delivery setup used for the sensor experiment.

facing the sensor array with the microprocessor, and the chamber containing five sensors. The microprocessor was installed on the LAB-X1 development board (MicroEngineering Labs, Inc.) equipped with an LCD text display, a small 4 × 4 keypad, and a serial port for data transfer. The board was equipped with an internal 5 V regulator that operated from either a 9 V battery or a plug-in power supply.

The PIC18F4550 microcontroller chip (Microchip Technology) included an on-chip multiplexed 10-bit A/D converter, and was operated at a modest clock rate of ca. 4 MHz. Note that power consumption and processing power in MIPS increase almost linearly with clock rate. Circuitry was built to convert the currents flowing through the sensor films to voltages read by the microprocessor. Each sensor channel consisted of a transimpedance amplifier, followed by a voltage inverter stage. Texas Instruments/Burr Brown OPA2703 dual operational amplifiers were used because of their low quiescent current requirement, low input bias current, low offset voltage, rail-to-rail output, and ability to operate from ±5 V power supplies. The schematic circuit diagram is shown in Fig. 2. The −5 V supply was derived from the +5 V using a commercial charge pump integrated circuit (not shown). All five channels were identical except that the transimpedance feedback resistors, which determined the electrical gain, were individually selected for the particular sensor due to the limited A/D converter resolution.

It should be noted that the LCD display did not include a backlight, and the current draw for the entire instrument, with the sensors operating, was ca. 25 mA. We ran the Mini-Mutt system continuously for several hours using a single 9 V battery and estimate that it could be battery-operated for at least 15 h without loss of performance. While a simple push button evaluation board was used for this configuration of the Mini-Mutt, a future generation could employ a backlit display with touch-screen control.

2.5. Data processing algorithm

The program was developed using the Microchip C compiler (MPLAB C18). A library of responses was prepared using the same vapors that would later be analyzed. The library was constructed by measuring the voltages from all five sensors simultaneously upon exposure to different concentrations of the analytes. Arrays of voltages versus concentration for each analyte were then stored into the microprocessor program. For determination of the identity and concentration of an unknown vapor presented to the system, an algorithm based on Eq. (2) was used. For each channel, the normalized resistance change ($\Delta R/R_o$) was calculated from the voltage reading in response to an analyte, in the preprocessing step, using:

$$\frac{\Delta R}{R_o}(\%) = \frac{R - R_o}{R_o} \times 100 = \frac{V_o - V}{V} \times 100 \quad (2)$$

where R is the resistance value at equilibrium of the sensor after exposure to the analyte, and R_o is the baseline resistance, and the V values are the corresponding output voltages (inversely proportional to the resistances). The proximity to each known vapor in the library was then computed by summing the squared difference of the normalized resistance change for the unknown analyte compared to each element of the library of known analytes; this procedure was performed for each of the five sensor channels. From these sums of squares (SOSs), the concentration with minimum SOS for each vapor was determined. The linearly interpolated points near this concentration were then examined to find the new minimum SOS. Using a self-limited stepwise recursive procedure, the process was repeated until the smallest SOS was found, and the analyte identity and its concentration were displayed on the LCD readout. The use of a

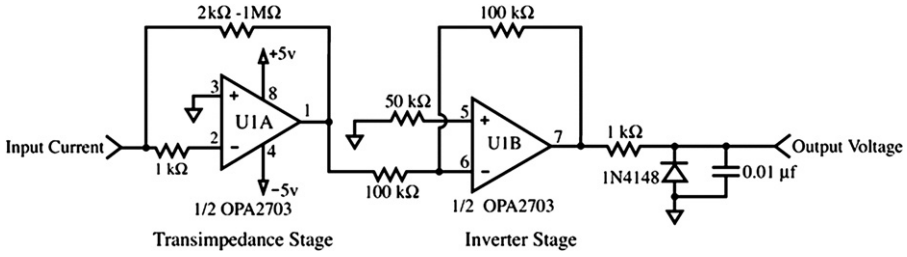

Fig. 2. Diagram of the current-to-voltage conversion circuit used to interface each sensor to the microprocessor.

Please cite this article in press as: J. Im, et al., A hybrid chemiresistive sensor system for the detection of organic vapors, Sens. Actuators B: Chem. (2011), doi:10.1016/j.snb.2011.02.025

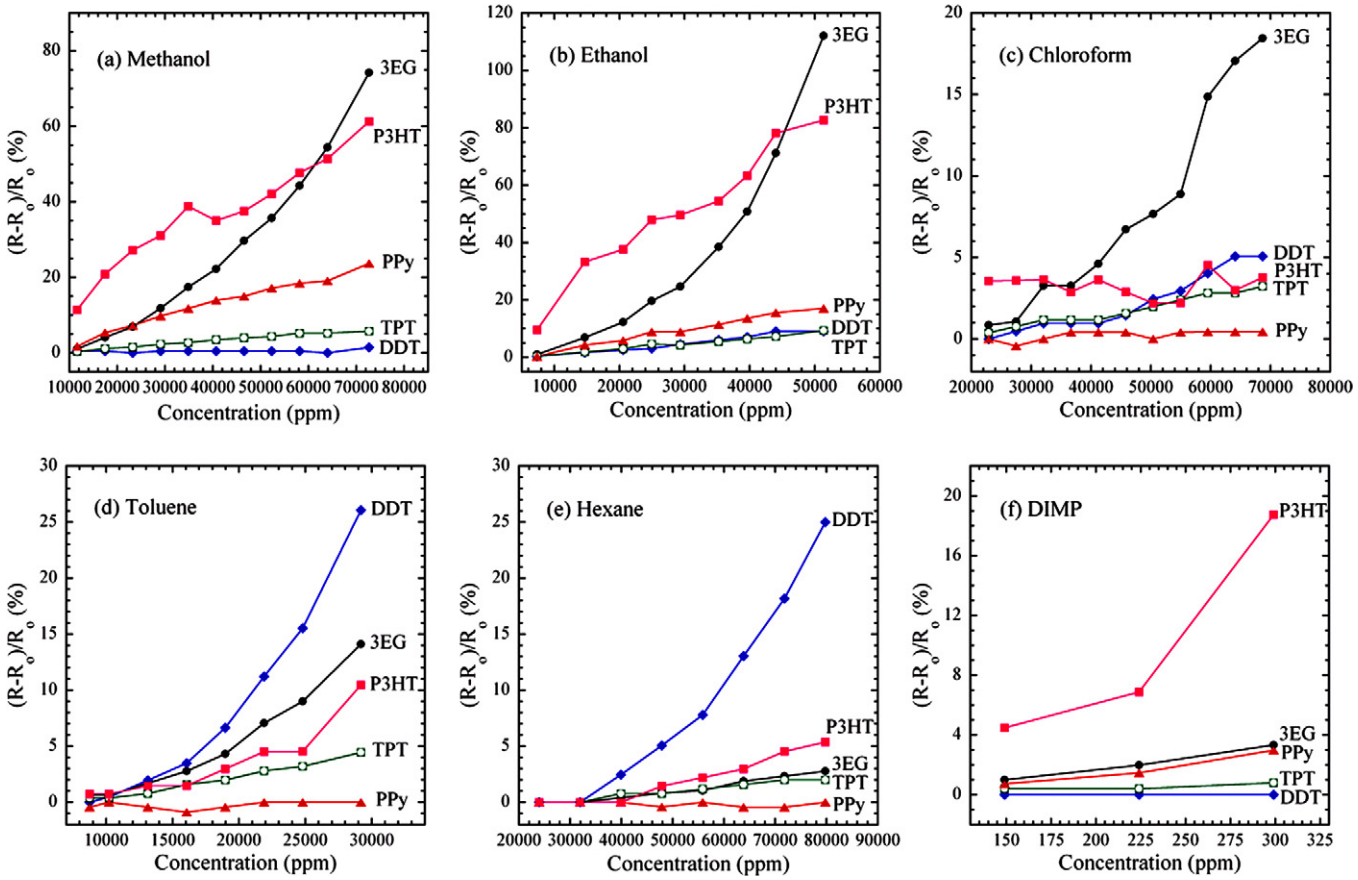

Fig. 3. Normalized electrical resistance changes of five chemiresistive sensor films in response to methanol, ethanol, chloroform, toluene, hexane, and DIMP vapors of varying concentration: 3EG: 3EG-AuNP, DDT: DDT-AuNP, TPT: TPT-AuNP, PPy: polypyrrole, and P3HT: poly(3-hexylthiophene) films.

computationally simple algorithm permits the use of a low-power and low-cost microcontroller for data acquisition and analysis.

2.6. Principal component analysis

Principal component analysis (PCA) was performed to estimate the response pattern of the sensor array using MATLAB 7.0. PCA enables visualization of multivariate data by reducing the dimensionality of a data set, while retaining most of the original information. Principal components (PCs) were calculated from the 5-by-5 covariance matrix of the data matrix (calibration data set) of 48 rows ($\Delta R/R_o$ in response to six analytes at different concentrations) by 5 columns (i.e., five sensors in an array).

3. Results and discussion

3.1. Properties of the sensor films

As discussed earlier, the sensor array consisted of five different sensing materials, including three different thiol-protected gold nanoparticle films (3EG-, DDT-, and TPT-AuNPs) and two conjugated polymer films (PPy and P3HT). Table 1 summarizes the properties of each sensor. The size distribution and interparticle (edge-to-edge) distance of the gold nanoparticles were measured by transmission electron microscopy. The 3EG-, DDT-, and TPT-AuNPs had mean core sizes of 4.9, 4.3, and 3.3 nm, respectively, with standard deviations of 1.3, 0.6, and 0.7 nm. The interparticle distances between the 3EG-, DDT-, and TPT-AuNPs gold cores were 1.5, 1.3, and 1.3 nm, respectively. Film thicknesses were measured using an atomic force microscope, and electrical conductivities of the five sensor films were calculated from Eq. (1). The electrical conductivity of the TPT-AuNP film was 5.75×10^{-4} S/cm, three orders of magnitude higher than that of the DDT-AuNP film. Considering the similar interparticle distances of TPT-AuNPs and DDT-AuNPs, the difference in electrical conductivities likely originates from the chemical structure of the thiol monolayer: the conjugated chain structure of TPT contributes to a higher probability of electron tunneling compared to the alkane chain of the DDT ligand. The electrical conductivity of the 3EG-AuNP film was similar to previously reported conductivities of monolayer-protected gold nanoparticles [34]. The conductivity of the polypyrrole film (doped with HCl) was 4.21×10^{-3} S/cm, while the conductivity of the undoped-P3HT film was 3.02×10^{-5} S/cm, two orders of magnitude lower than that of the polypyrrole film. For P3HT films, it is known that oxygen causes p-doping [35].

3.2. Vapor sensor responses

To build a library of sensor responses, the sensor array was exposed to an analyte at a series of concentrations, while simultaneously measuring the electrical resistances of the five sensors. Six different vapors were chosen as analytes: methanol, ethanol, chloroform, toluene, hexane, and diisopropyl methylphosphonate (DIMP). The sensor array was exposed to each analyte vapor for 3 min to allow the resistance to stabilize. The response was reversible in all cases, typically returning to within 5% of the initial value. Fig. 3 shows the response of the sensor array to the six analytes at varying concentrations. In all cases, the resistivities of the films increased upon exposure to vapors. In the case of the

Please cite this article in press as: J. Im, et al., A hybrid chemiresistive sensor system for the detection of organic vapors, Sens. Actuators B: Chem. (2011), doi:10.1016/j.snb.2011.02.025

Table 2
Responses and recovery times of the five sensor films.

Sensor	Response time[a]	Recovery time[b]
3EG-AuNPs	2 min, 24 s (±14%)	1 min, 56 s (±29%)[c]
DDT-AuNPs	2 min, 27 s (±9%)	54 s (±1%)[c]
TPT-AuNPs	2 min (±20%)	1 min, 17s (±34%)[c]
PPy	2 min (±45%)	49 s (±22%)[d]
P3HT	1 min, 45 s (±56%)	Highly variable: 1–14 min[c]

[a] Time at which the response reaches 90% of the saturated (equilibrium) value.
[b] Time at which 90% of the response is recovered.
[c] Average recovery time, except for the time in response to DIMP vapor.
[d] Average recovery time, except for the time in response to ethanol vapor.

gold nanoparticles, this behavior may be attributed to swelling of the film, which increases the interparticle distance between gold cores. For the conjugated polymers, swelling leads to an increase in the distance between polymer backbone chains, thereby increasing the energy barrier for electron hopping and decreasing the charge carrier mobility. Absorption of analyte molecules can also cause de-doping of the polymer film by hindering carrier mobility along the backbone chain, thereby increasing electrical resistance [35].

Table 2 summarizes response and recovery times of the sensor films when exposed to vapors. The former is defined as the time needed for the resistance to reach 90% of the equilibrium value, and the latter is the time necessary to return to 90% of the value read prior to exposure. We estimate that 17 s were required to saturate the chamber with analyte vapor due to its dead volume. As seen in the table, the values varied greatly depending on the sensor and analyte. However, the response time of the sensor films was, on average, 2 min. P3HT showed greater variation in its recovery times compared to the other sensor films. While it exhibited rapid recovery (1–2 min) after exposure to alcohol analytes (i.e., ethanol and methanol), the recovery times for toluene, hexane and DIMP were 6, 14, and 37 min, respectively.

Fig. 4 displays sensitivity factors of the five sensors in response to six different analytes. The sensitivity factor was calculated from the slopes of linear fits through the lower concentration regions of the data in Fig. 3, where the normalized resistance changes were essentially linear with respect to concentration. It is worth noting that the sensitivity factors in response to DIMP vapor were more than 30 times higher than those to the others, except for DDT-AuNPs. In particular, the P3HT film showed very strong response to DIMP vapor among the five sensors, which was two times stronger than the responses of the 3EG-AuNP and polypyrrole films. The sensitivity of the TPT-AuNP film to DIMP vapor was 10 times smaller than that of the P3HT film. In contrast, the DDT-AuNP film showed no response to DIMP vapor. The P3HT sensor, as well as the 3EG-AuNP film, showed strong response to methanol and ethanol vapors.

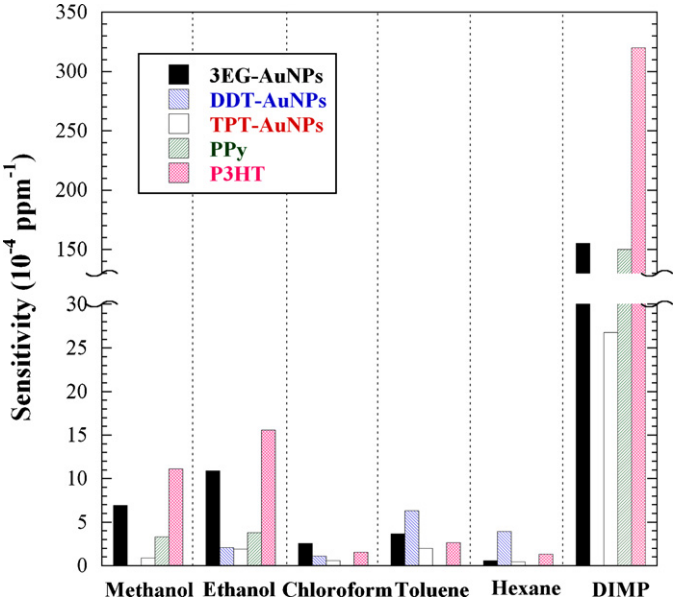

Fig. 4. Sensitivity factors of the five sensor films responding to six chemical vapors. The *x*-axis represents the analtyes examined in the sensor measurements: methanol, ethanol, chloroform, toluene, hexane, and DIMP vapors. The *y*-axis represents the sensitivity factor of each film to the analyte, calculated from the slope of a linear fit in the lower concentration region of Fig. 3. Spaces in the *y*-axis and in the columns indicate breaks between 30×10^{-4} and 150×10^{-4} ppm^{-1}.

Table 3
Sensitivity orders of five sensor installed in an array.

Sensor	Sensitivity order
3EG-AuNPs	DIMP ≫ ethanol > methanol > toluene > chloroform > hexane
DDT-AuNPs	Toluene > hexane > ethanol > chloroform ≫ methanol = DIMP (no response)
TPT-AuNPs	DIMP ≫ toluene > ethanol > methanol > chloroform > hexane
PPy	DIMP ≫ ethanol > methanol ≫ chloroform = toluene = hexane (no response)
P3HT	DIMP ≫ ethanol > methanol > toluene > chloroform > hexane

Table 3 summarizes the sensitivity order of the five sensors installed in the Mini-Mutt in response to the six analytes. Note that the DDT-AuNP sensor responded strongly to the nonpolar vapors (toluene and hexane) and exhibited no response to methanol and DIMP vapors. On the other hand, the polypyrrole film showed strong response to DIMP, ethanol, and methanol, and no response to chloroform, toluene, and hexane vapors.

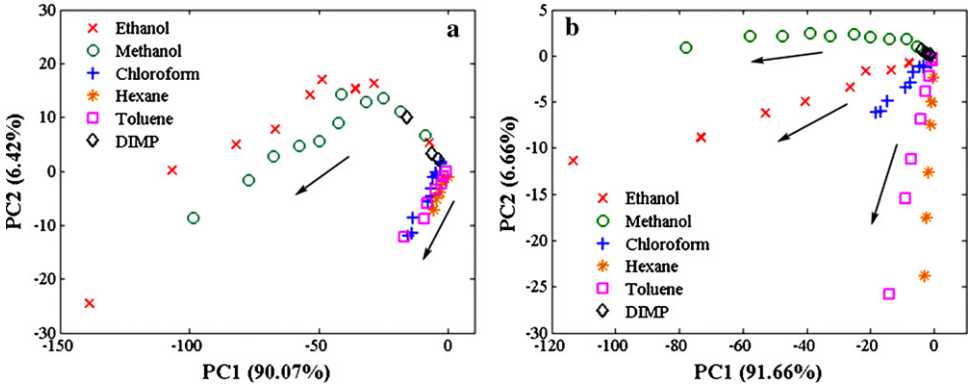

Fig. 5. Results of principal component analysis of a sensor array for six analytes: (a) PCA results from the five sensors installed in the array including 3EG-, DDT-, TPT-AuNPs, PPy, and P3HT films and (b) PCA results from the four sensors including 3EG-, DDT-, TPT-AuNPs, and PPY films, with exclusion of the P3HT film.

Please cite this article in press as: J. Im, et al., A hybrid chemiresistive sensor system for the detection of organic vapors, Sens. Actuators B: Chem. (2011), doi:10.1016/j.snb.2011.02.025

Table 4
Test results of the sensor array for identification/quantification of the six vapors.

Test analyte and its concentration (ppm)	Predicted analyte and its concentration (ppm) with SOS[a]		
	1st prediction	2nd prediction	3rd prediction
Toluene			
18,970	Toluene, 2042 (12.4)		
21,888	Toluene, 21,888 (64.6)		
24,807	Toluene, 24,442 (66.5)		
26,996	Toluene, 26,996 (38.3)		
Ethanol			
7335	DIMP, 299 (4.2)	Ethanol, 9169 (7.7)	
29,342	Ethanol, 39,612 (1467.5)		
44,013	Ethanol, 45,847 (3535.0)		
Chloroform ($CHCl_3$)			
22,893	Toluene, 11,674 (0.3)	DIMP, 149 (0.6)	$CHCl_3$, 24,037 (1.6)
45,786	$CHCl_3$, 57,233 (13.1)		
64,101	$CHCl_3$, 68,679 (76.5)		
Hexane			
39,888	Toluene, 10,214 (2.6)	Hexane, 39,888 (8.8)	
63,821	Toluene, 18,970 (15.3)	Hexane, 53,849 (17.3)	
79,776	Hexane, 67,810 (42.1)		
Methanol			
11,628	Methanol, 15,988 (5.3)		
40,697	Ethanol, 30,809 (269.4)	Methanol, 53,777 (603.6)	
63,952	Ethanol, 44,013 (322.4)	Methanol, 72,673 (829.3)	
DIMP			
149	DIMP, 224 (0.1)		
299	Ethanol, 22,740 (241.1)	Methanol, 34,883 (408.9)	DIMP, 299 (1088.1)

[a] SOS (the value in parenthesis) represents the sum of the squares of the differences between measured responses and the library responses for all of the sensors.

3.3. Principal component analysis

Principal component analysis (PCA) was performed to determine the response pattern of the sensor array. Fig. 5(a) exhibits the results of principal component analysis for the array of the five sensing films in response to six analytes at different concentrations. The first principal component (PC1) accounted for the largest percentage of the total variability, and the second PC (PC2) accounted for the next largest percentage. The first two PCs presented a high cumulative variance of 96.49%. As shown in the figure, ethanol and methanol vapors were well-separated from the relatively nonpolar chloroform, hexane and toluene vapors; however, they overlapped with DIMP vapor in the lower concentration range. Fig. 5(b) displays the PCA results for the use of four sensors: 3EG-, DDT-, TPT-AuNPs, and PPy films. In this case, the cumulative variance of the first two PCs was 98.32%. When the P3HT sensor was not used, the sensor array with four sensors showed sufficient recognition ability toward the target vapors, except that the DIMP vapor overlapped at low methanol concentration. These results demonstrate that the performance of a sensor array can be altered by varying the configured choice of sensors and indicate that incorporation of PCA into the detection algorithm could enhance the classification and identification abilities of the sensor array.

3.4. Long-term stability of the sensors

The library derived from the data shown in Fig. 3 was used for calibration of the sensor array. After 1 month, it was tested at several vapor concentrations that had originally been used to construct the library. Table 4 summarizes the results of these experiments. The algorithm was modified to show the three possible analytes in the order of the smallest sum of the squares of the differences between measured response and library response (i.e., calibration data set) for all the sensors. The sensor array exhibited excellent ability to detect toluene, hexane and chloroform vapors, with correct concentrations displayed on the LCD screen and with R^2 values of 0.97, 0.98 and 0.95, respectively. However, the sensor array showed degraded performance after a month with respect to ethanol, methanol, and DIMP vapors at the lower concentrations. This is mainly due to instability of the P3HT film, and it was found that the baseline resistance of the undoped-P3HT film varied with time, perhaps due to oxygen doping from gas dissolved in the ana-

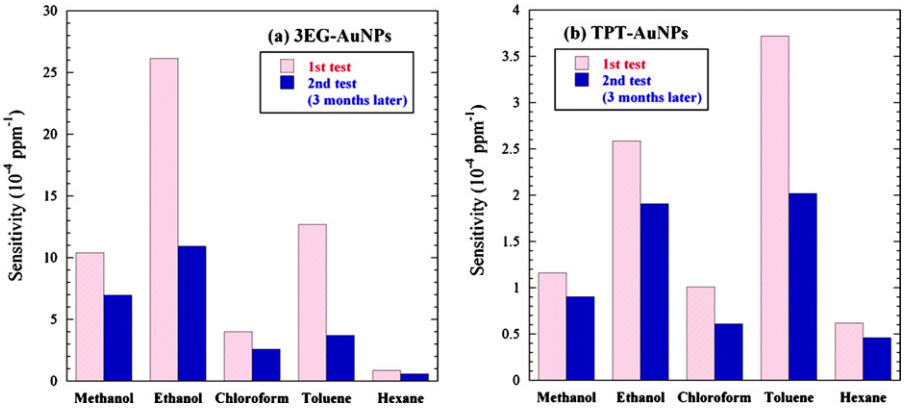

Fig. 6. Comparison of sensitivity factors of the two gold nanoparticle sensors after three months of use: (a) 3EG-AuNP and (b) TPT-AuNP films.

Please cite this article in press as: J. Im, et al., A hybrid chemiresistive sensor system for the detection of organic vapors, Sens. Actuators B: Chem. (2011), doi:10.1016/j.snb.2011.02.025

lytes. In light of the higher sensitivities of P3HT with respect to ethanol, methanol, and DIMP vapors (shown in Fig. 4), compared to the other sensors, instability of the P3HT apparently contributed strongly to this irreproducibility.

The 3EG- and TPT-AuNP films were used for a total of 3 months for the sensor measurements, without replacement. Fig. 6 summarizes the long-term stability of two of the gold nanoparticle sensor films. In the case of the 3EG-AuNP film, the sensitivity factor decreased from 30% to 71% (depending on the analyte) after three months of use and storage at ambient conditions. The sensitivity order of the 3EG-AuNP film was ethanol > toluene > methanol > chloroform > hexane. After three months, the sensitivity order changed to: ethanol > methanol > toluene > chloroform > hexane. For the TPT-AuNP film, the sensitivity factor decreased from 22% to 46% (depending on the analyte), and the sensitivity order remained toluene > ethanol > methanol > chloroform > hexane. These results suggest that the TPT-AuNP film is more stable than the 3EG-AuNP film.

Possible reasons for the reduced sensitivity of the films include deterioration due to oxygen, water, and/or ozone, and aging after many cycles of measurements. Joseph et al. [36] reported aging of 1,ω-alkyldithiol-interlinked gold nanoparticle networks, mainly due to oxidation of the thiols in the presence of oxygen, ozone and light, which affected sensor performance. In our study, the sensors were stored in a light-shielded chamber, but environmental oxygen and moisture were not excluded. The sensors were exposed to high concentrations of analytes for a total of 7 h during three months. XPS analysis of the 3EG- and TPT-AuNP films was carried out to investigate film aging. The S2p spectra of the gold nanoparticle films (not shown) indicated that a fraction of the thiolate peaks (occurring at 163 eV) were oxidized, with a binding energy of 169 eV. It is therefore likely that partial desorption and decomposition of the thiol monolayer occurred due to organic vapor exposure.

4. Conclusions

We have demonstrated a portable, battery-operated, microprocessor-based prototype multi-sensor array system based on three different thiol-monolayer protected gold nanoparticles and two conjugated polymers for detection of organic vapors and a nerve agent simulant. This work is the first demonstration of a hybrid array of thiol-monolayer protected gold nanoparticles in combination with conjugated polymers. Calibration was carried out from a response library of the sensor array to six analytes at different concentrations. The measurements were performed simultaneously, permitting direct comparison of sensitivity and response and recovery times. Overall, it was observed that sensor films responded, with greatest sensitivity, to organic analytes with similar chemical functionality (e.g., polarity). The colloidal gold nanoparticle films generally exhibited faster recovery times than the poly(3-hexylthiophene) film. An algorithm based on "minimization of squares of the differences" method was tested to discriminate and identity target vapors. The prototype sensor system showed excellent identification and quantification of toluene, but poorer results, due to long-term stability issues for the other analytes. Future work will concentrate on adding a miniaturized array of a larger number of sensors and on more sophisticated algorithms.

Acknowledgement

This work was supported by a multi-sensor grant from the Army Research Laboratory to the University of Massachusetts Lowell. The views expressed in this article are not necessarily endorsed by the sponsor.

References

[1] K.J. Albert, N.S. Lewis, C.L. Schauer, G.A. Sotzing, S.E. Stitzel, T.P. Vaid, D.R. Walt, Cross-reactive chemical sensor arrays, Chem. Rev. 100 (2000) 2595–2626.
[2] K.A. Ngo, P. Lauque, K. Aguir, High performance of a gas identification system using sensor array and temperature modulation, Sens. Actuators B 124 (2007) 209–216.
[3] P.C. Chen, F.N. Ishikawa, H.K. Chang, K. Ryu, C. Zhou, A nanoelectronic nose: a hybrid nanowire/carbon nanotube sensor array with integrated micromachined hotplates for sensitive gas discrimination, Nanotechnology 20 (2009) 125503 (1–8).
[4] S. Maldonado, E.G. Berríos, M.D. Woodka, B.S. Brunschwig, N.S. Lewis, Detection of organic vapors and NH_3(g) using thin-film carbon black-metallophthalocyanine composite chemiresistors, Sens. Actuators B 134 (2008) 521–531.
[5] M.S. Freund, N.S. Lewis, A chemically diverse conducting polymer-based "electronic nose", Proc. Natl. Acad. Sci. 92 (1995) 2652–2656.
[6] J.B. Chang, V. Lu, V. Subramanian, K. Sivula, C. Luscombe, A. Murphy, J. Liu, J.M.J. Fréchet, Printable polythiophene gas sensor array for low-cost electronic noses, J. Appl. Phys. 100 (2006) 014506 (1–7).
[7] B. Li, S. Santhanam, L. Schultz, M.J. El, M.C. Iovu, G. Sauvé, J. Cooper, R. Zhang, J.C. Revelli, A.G. Kusne, J.L. Snyder, T. Kowalewski, L.E. Weiss, R.D. McCullough, G.K. Fedder, D.N. Lambeth, Inkjet printed chemical sensor array based on polythiophene conductive polymers, Sens. Actuators B 123 (2007) 651–660.
[8] L.R. Khot, S. Panigrahi, P. Sengupta, Development and evaluation of chemoresistive polymer sensors for low concentration detection of volatile organic compounds related to food safety applications, Sens. Instrum. Food Qual. 4 (2010) 20–34.
[9] B.J. Doleman, M.C. Lonergan, E.J. Severin, T.P. Vaid, N.S. Lewis, Quantitative study of the resolving power of arrays of carbon black-polymer composites in various vapor-sensing tasks, Anal. Chem. 70 (1998) 4177–4190.
[10] S.V. Patel, M.W. Jenkins, R.C. Hughes, W.G. Yelton, A.J. Ricco, Differentiation of chemical components in a binary solvent vapor mixture using carbon/polymer composite-based chemiresistors, Anal. Chem. 72 (2000) 1532–1542.
[11] D. Rivera, M.K. Alam, C.E. Davis, C.K. Ho, Characterization of the ability of polymeric chemiresistor arrays to quantitate trichloroethylene using partial least squares (PLS): effects of experimental design, humidity, and temperature, Sens. Actuators B 92 (2003) 110–120.
[12] T. Gao, E.S. Tillman, N.S. Lewis, Detection and classification of volatile organic amines and carboxylic acids using arrays of carbon black-dendrimer composite vapor detectors, Chem. Mater. 17 (2005) 2904–2911.
[13] T. Alizadeh, Chemiresistor sensors array optimization by using the method of coupled statistical techniques and its application as an electronic nose for some organic vapors recognition, Sens. Actuators B 143 (2010) 740–749.
[14] N. Elfström, K. Eriksson, A. Karlström, J. Linnros, Silicon nanoribbons for electrical detection of biomolecules, Nano Lett. 8 (2008) 945–949.
[15] S. Clavaguera, A. Carella, L. Caillier, C. Celle, J. Pécaut, S. Lenfant, D. Vuillaume, J.P. Simonato, Sub-ppm detection of nerve agents using chemically functionalized silicon nanoribbon field-effect transistors, Angew. Chem. Int. Ed. 49 (2010) 4063–4066.
[16] H. Wohltjen, A.W. Snow, Colloidal metal–insulator–metal ensemble chemiresistor sensor, Anal. Chem. 70 (1998) 2856–2859.
[17] Y. Joseph, B. Guse, T. Vossmeyer, A. Yasuda, Gold nanoparticle/organic networks as chemiresistor coatings: the effect of film morphology on vapor sensitivity, J. Phys. Chem. C 112 (2008) 12507–12514.
[18] Q.Y. Cai, E.T. Zellers, Dual-chemiresistor GC detector employing monolayer-protected metal nanocluster interfaces, Anal. Chem. 74 (2002) 3533–3539.
[19] L. Han, X. Shi, W. Wu, F.L. Kirk, J. Luo, L. Wang, D. Mott, L. Cousineau, S.I. Lim, S. Lu, C.J. Zhong, Nanoparticle-structured sensing array materials and pattern recognition for VOC detection, Sens. Actuators B 106 (2005) 431–441.
[20] C.Y. Yang, C.L. Li, C.J. Lu, A vapor selectivity study of microsensor arrays employing various functionalized ligand protected gold nanoclusters, Anal. Chim. Acta 565 (2006) 17–26.
[21] W.H. Steinecker, M.P. Rowe, E.T. Zellers, Model of vapor-induced resistivity changes in gold-thiolate monolayer-protected nanoparticle sensor films, Anal. Chem. 79 (2007) 4977–4986.
[22] L. Wang, X. Shi, N.N. Kariuki, M. Schadt, G.R. Wang, Q. Rendeng, J. Choi, J. Luo, S. Lu, C.J. Zhong, Array of molecularly mediated thin film assemblies of nanoparticles: correlation of vapor sensing with interparticle spatial properties, J. Am. Chem. Soc. 129 (2007) 2161–2170.
[23] J.S. Cooper, B. Raguse, E. Chow, L. Hubble, K.H. Muller, L. Wieczorek, Gold nanoparticle chemiresistor sensor array that differentiates between hydrocarbon fuels dissolved in artificial seawater, Anal. Chem. 82 (2010) 3788–3795.
[24] H. Ahn, A. Chandekar, B. Kang, C. Sung, J.E. Whitten, Electrical conductivity and vapor-sensing properties of ω-(3-thienyl)alkanethiol-protected gold nanoparticle films, Chem. Mater. 16 (2004) 3274–3278.
[25] J. Im, A. Chandekar, J.E. Whitten, Anomalous vapor sensor response of a fluorinated alkylthiol-protected gold nanoparticle film, Langmuir 25 (2009) 4288–4292.
[26] J.W. Gardner, J. Yinon, Electronic Noses and Sensors for the Detection of Explosives, Kluwer Academic Publishers, Dordrecht/Boston/London, 2000, pp. 1–28.
[27] A.W. Snow, H. Wohltjen, N.L. Jarvis, MIME chemical vapor microsensors, in: J.D. Bultman (Ed.), 2002 NRL Review, Naval Research Laboratory, Washington, D.C., 2002, pp. 45–55, this is also available at: http://www.nrl.navy.mil/content.php?P=02REVIEW45.

Please cite this article in press as: J. Im, et al., A hybrid chemiresistive sensor system for the detection of organic vapors, Sens. Actuators B: Chem. (2011), doi:10.1016/j.snb.2011.02.025

[28] A.D. Wilson, M. Baietto, Applications and advances in electronic-nose technologies, Sensors 9 (2009) 5099–5148.
[29] M.G. Ancona, A.W. Snow, E.E. Foos, W. Kruppa, R. Bass, Scaling properties of gold nanocluster chemiresistor sensors, IEEE Sens. J. 6 (2006) 1403–1414.
[30] K.E. Kramer, S.L. Rose-Pehrsson, K.J. Johnson, C.P. Minor, Hybrid arrays for chemical sensing, in: M.A. Ryan, A.V. Shevade, C.J. Taylor, M.L. Homer, M. Blanco, J.R. Stetter (Eds.), Computational Methods for Sensor Material Selection, Springer, New York, 2009, pp. 265–298, Chapter 12.
[31] M. Brust, M. Walker, D. Bethell, D.J. Schiffrin, R. Whyman, Synthesis of thiol-derivatized gold nanoparticles in a two-phase liquid–liquid system, J. Chem. Soc. Chem. Commun. 7 (1994) 801–802.
[32] X. Zhang, S.K. Manohar, Bulk synthesis of polypyrrole nanofibers by a seeding approach, J. Am. Chem. Soc. 126 (2004) 12714–12715.
[33] H. Wohltjen, W.R. Barger, A.W. Snow, N.L. Jarvis, A vapor-sensitive chemiresistor fabricated with planar microelectrodes and a Langmuir–Blodgett organic semiconductor film, IEEE Trans. Electron Dev. ED-32 (1985) 1170–1174.
[34] E.E. Foos, A.W. Snow, M.E. Twigg, M.G. Ancona, Thiol-terminated di-, tri-, and tetraethylene oxide functionalized gold nanoparticles: a water-soluble, charge-neutral cluster, Chem. Mater. 14 (2002) 2401–2408.
[35] H.H. Liao, C.M. Yang, C.C. Liu, S.F. Horng, H.F. Meng, J.T. Shy, Dynamics and reversibility of oxygen doping and de-doping for conjugated polymer, J. Appl. Phys. 103 (2008) 104506 (1–8).
[36] Y. Joseph, B. Guse, G. Nells, Aging of 1,ω-alkyldithiol interlinked Au nanoparticle networks, Chem. Mater. 21 (2009) 1670–1676.

Biographies

Jisun Im is a PhD candidate in the polymer science program in the Department of Chemistry at the University of Massachusetts Lowell. She received her bachelor of science and master of science degrees in polymer science and engineering at Pusan National University in South Korea for work on organic–inorganic hybrid nanocomposites. Her present research interests include metal oxide surface chemistry and sensors.

Sandip K. Sengupta is a senior scientist at the University of Massachusetts Lowell. He has many research interests, including conjugated polymers, nanomanufacturing, low-cost spectroscopy experiments, and surface science. He is also an expert at electronics and sensors.

Maor F. Baruch is a chemistry major at the University of Massachusetts Lowell. He is planning to attend graduate school to pursue a PhD in Chemistry.

Christopher D. Granz obtained a double major in electrical engineering and computer science at the University of Massachusetts Lowell, where he is now pursuing his MS in computer science.

Srikanth Ammu is a PhD candidate in chemical engineering at the University of Massachusetts Lowell. His areas of interest include chemical sensors.

Professor Sanjeev K. Manohar is an associate professor in the Department of Chemical Engineering at the University of Massachusetts Lowell. He received his PhD from the University of Pennsylvania in 1992. He is an expert in conjugated polymers, nanostructured materials for energy and biomedical applications, and chemical sensors.

Professor James E. Whitten is a professor and chair of the Department of Chemistry at the University of Massachusetts Lowell. He received his PhD from Ohio State University in 1991 and performed postdoctoral research at the University of Chicago. His areas of expertise include polymer–metal interfaces, organic electronics, photoelectron spectroscopy, metal oxides, self-assembled monolayers, chemical sensors, and low-cost spectroscopy experiments for chemical education.

Please cite this article in press as: J. Im, et al., A hybrid chemiresistive sensor system for the detection of organic vapors, Sens. Actuators B: Chem. (2011), doi:10.1016/j.snb.2011.02.025